Antiphase boundaries in improper ferroelastic crystals: orientation and transformation of boundary structure

1991 J. Phys.: Condens. Matter 3 7117

(http://iopscience.iop.org/0953-8984/3/37/002)

J. Phys.: Condens. Matter 3 (1991) 7117–7128. Printed in the UK

Antiphase boundaries in improper ferroelastic crystals: orientation and transformation of boundary structure

I Rychetsky
Institute of Physics, Czechoslovak Academy of Sciences, Na Slovance 2, 18040 Prague, Czechoslovakia

Received 10 January 1991

Abstract. Thick antiphase boundaries (APB) in improper ferroelastic crystals are studied in the framework of the Landau expansion. Making use of the compatibility restrictions, two qualitatively different types of boundaries are predicted. The stress-free ones have preferred temperature-dependent orientations, for which an explicit formula is calculated. The strained boundaries, in contrast, possess non-mechanical stress along the boundary plane also in the crystallographic lock-in orientation with minimum energy. The transition between linear and rotational APB structures can appear as a minimum in the preferred APB orientation versus temperature curve. Consequently, the linear and orientational structures can be distinguished as well as determination of the APB transition temperature. A comparison with experimental observations is given.

1. Introduction

Some improper ferroelastics, e.g. $Gd_2(MoO_4)_3$ (GMO), Hg_2Cl_2 and KSCN, undergo a phase transition with symmetry breaking from tetragonal to orthorhombic and doubling of the unit cell. In the low-temperature phase two types of domain walls can exist. Ferroelastic domain walls are formed between domains of different macroscopic states characterized by different strain tensors. Their coherent orientations are determined by the crystal symmetry and coincide with two mirror planes lost at the transition. The second type is an antiphase boundary (APB) joining two domains of identical strain tensors with structures mutually shifted by a translation lost at the transition. Consequently, all APB orientations are coherent but may still be energetically non-equivalent. The APB in GMO have been observed by several authors. Meleshina *et al* [1] using an etching method observed closed-loop boundaries and also boundaries beginning and terminating (see [2]) at ferroelastic walls or dislocations. All APB orientations appeared in the sample but one of them was clearly preferred. The APB of the preferred orientation are probably boundaries with the lowest energy. Barkley and Jeitschko [3] pulled such boundaries out from dislocations by a moving ferroelectric and ferroelastic domain wall and then visualized them by chemical etching. The temperature dependence of the preferred APB orientation was measured. The etching method, as well as observations in GMO performed by Yamamoto *et al* [4] using electron microscopy and by Malgrange and Capelle [5] by x-ray topography, did not reveal any details of the internal boundary structure. On the basis of experimental data [3], Capelle and Malgrange [6] have

0953-8984/91/377117 + 12 $03.50

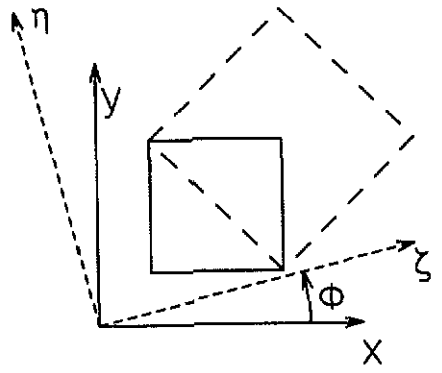

Figure 1. The square (———) represents a tetragonal cell; the rectangle (– – –) is an orthorhombic cell; x, y are axes of the tetragonal phase, while ζ, η are axes perpendicular and parallel, respectively, to the APB.

estimated the boundary thickness to be of the order 100–1000 Å, i.e. about 20–200 lattice constants. This supports the continuum approach to the APB.

From the theoretical point of view, two qualitatively different types of APB exist. In the linear one the spontaneous strain tensor component has the same sign throughout the boundary. On the other hand, in the rotational APB that component changes its sign at the boundary centre and, therefore, a nucleus of a ferroelastic layer domain appears inside the APB. Full saturation of the central domain leads to a splitting of the APB into two ferroelastic walls. Several authors [7–10] theoretically investigated the transition between linear and rotational APB structures without taking into account deformations. The rotational and linear structures have not been distinguished in experimentally observed APB [1, 3–5] since the boundary width is too small.

Recently, some elastic properties of APB and ferroelastic domain walls in improper ferroelastic crystals with the perovskite structure, e.g. $SrTiO_3$, were theoretically studied [11]. It was shown that the walls are generally three-dimensional objects rather than quasi-one-dimensional ones, but their profiles were not calculated. It was shown that quasi-one-dimensional domain walls can exist under an appropriate applied non-homogeneous external stress.

The paper is organized as follows. In section 2 the phenomenological description of the Hg_2Cl_2 crystal is presented and the role of crystal symmetry and topology is pointed out. In section 3 the linear and rotational APB, as well as the phase transition inside the APB, are reviewed without strains being taken into account. In section 4 the APB with compatible deformations is studied, the temperature dependence of the boundary orientation is calculated, and the stress-free boundaries and the APB possessing non-mechanical internal stress are analysed. The results are compared with experiments in section 5.

2. The free energy

We shall consider the improper ferroelastic crystal Hg_2Cl_2 (and isomorphous mercurous halides Hg_2Br_2 and Hg_2I_2) undergoing a phase transition from the tetragonal phase with space group D_{4h}^{17} ($I4/mmm$) to the orthorhombic phase with doubled unit cell (figure 1) and D_{2h}^{17} ($Cmcm$) space group [12]. In the high-temperature phase the single crystal is built up of parallel chains along the z axis of weakly bound linear molecules Cl–Hg–Hg–Cl with one molecule in the primitive unit cell. The transverse acoustic soft modes of the

transition have wavevectors $\boldsymbol{K}(X_1)$ and $\boldsymbol{K}(X_2)$ determined by two non-equivalent X-points of the Brillouin zone, $X_1 = (\frac{1}{2}a, \frac{1}{2}a, 0)$ and $X_2 = (\frac{1}{2}a, -\frac{1}{2}a, 0)$. These modes are polarized in the xy plane and correspond to displacements of the centres of gravity of the molecules perpendicular to the z axis. The strong anisotropy of the chain structure and the physical properties (elastic moduli, birefringence, etc) of the crystal, together with the fact that the phase transition is induced by the soft mode lying (i.e. its $\boldsymbol{K}$ vector and polarization) in the xy plane, indicate that the two-dimensional approximation could be adequate. We shall therefore assume that the only non-zero strain tensor components are u_{xx}, u_{yy} and u_{xy}. The axes x, y are that of the tetragonal structure, while ζ, η are other ones rotated through an angle φ.

The free energy density expansion can be written as a sum of three parts:

$$f = f_0 + f_i + f_a. \tag{1}$$

The main contribution to energy is f_0 [12]:

$$f_0 = \tfrac{1}{2}t(p^2+q^2) + \tfrac{1}{4}\beta'(p^2-q^2)^2 + \tfrac{1}{2}\gamma' p^2q^2 + \tfrac{1}{2}\kappa[(\nabla p)^2 + (\nabla q)^2] + l_6'(p^2-q^2)u_6 + l_1'(p^2+q^2)(u_1+u_2) + \tfrac{1}{2}\sum c_{ij}u_iu_j - \sum \sigma_i u_i \tag{2}$$

where p, q is a two-component order parameter, and $t = a(T - T_C)$. For tensor components, the contracted notation is used: $xx = 1, yy = 2, zz = 3, yz = 4, zx = 5, xy = 6$; σ_i is the stress tensor and c_{ij} are elastic constants.

The last two parts in (1) involve higher-order terms in comparison with f_0. They are given by the following expressions:

$$f_i = r_1'(u_1+u_2)[(\nabla p)^2 + (\nabla q)^2] + r_6'u_6[(\nabla p)^2 - (\nabla q)^2] + \kappa_1[(\nabla p)^2 + (\nabla q)^2]^2 + t_1'(u_1+u_2)(p^2+q^2)^2 + t_6'u_6(p^2+q^2)(p^2-q^2) + k_1'(u_1+u_2)p^2q^2 + \bar{t}_1(p^2+q^2)^3 + \bar{t}_6(p^2+q^2)(p^2-q^2)^2 + \bar{k}_1(p^2+q^2)p^2q^2 \tag{3}$$

and

$$f_a = s_6'u_6(\partial_x p\,\partial_y p + \partial_x q\,\partial_y q) + \kappa_2[(\partial_x p\,\partial_y q)^2 + (\partial_x q\,\partial_y p)^2] + \kappa_3\,\partial_x p\,\partial_y p\,\partial_x q\,\partial_y q + \kappa_4[(\partial_x p)^4 + (\partial_y p)^4 + (\partial_x q)^4 + (\partial_y q)^4] + \bar{s}_6(p^2-q^2)(\partial_x p\,\partial_y p + \partial_x q\,\partial_y q). \tag{4}$$

In a unidirectional modulation, the special case of which is a planar domain wall, the order parameter is a function of only one space coordinate ζ: $p(\zeta), q(\zeta)$. The direction of the ζ axis is a general one for the present. The boundary plane is perpendicular to ζ and its orientation is determined by the angle φ (see figure 1). We should realize that the rotated coordinate system ζ, η is tied to the direction of modulation, while x, y are the tetragonal axes of the crystal itself. So, in order to rotate the modulation inside the crystal, only the derivatives have to be transformed while the strain tensor components are fixed in x, y coordinate system. The relations between the rotated coordinate systems are

$$\zeta = x\cos\varphi + y\sin\varphi \qquad \eta = -x\sin\varphi + y\cos\varphi. \tag{5}$$

Then the gradient terms in f_0 and f_i can be written in the form: $(\nabla p)^2 = (\mathrm{d}_\zeta p)^2$ and $(\nabla q)^2 = (\mathrm{d}_\zeta q)^2$. Hence it follows that f_0 and f_i are fully isotropic with respect to the

modulation orientation in the crystal as they do not depend on φ. The term f_a is changed to

$$f_a = \tfrac{1}{2}[s_6' u_6 + \bar{s}_6(p^2 - q^2)][(\mathrm{d}_\zeta p)^2 + (\mathrm{d}_\zeta q)^2]\sin(2\varphi) + \tfrac{1}{4}\{\kappa_4[(\mathrm{d}_\zeta p)^4 + (\mathrm{d}_\zeta q)^4] - \tfrac{1}{2}(2\kappa_2 + \kappa_3)(\mathrm{d}_\zeta p\,\mathrm{d}_\zeta q)^2\}\cos(4\varphi) + \tfrac{3}{4}\kappa_4[(\mathrm{d}_\zeta p)^4 + (\mathrm{d}_\zeta q)^4] + \tfrac{1}{4}(2\kappa_2 + \kappa_3)(\mathrm{d}_\zeta p\,\mathrm{d}_\zeta q)^2. \quad (6)$$

The angle φ appears in (6) and therefore the term f_a represents the part of the free energy crystallographically anisotropic with respect to the modulation orientation φ. In fact, below the phase transition a unidirectional modulation of the orthorhombic phase can appear. Then the terms before the sine and cosine are non-zero and two crystallographic directions have extreme energy density, $\varphi = \pi/4$, $\varphi = -\pi/4$, as can be obtained by differentiating (6) with respect to φ. These directions correspond to two mirror planes of the orthorhombic phase. If the cosine term coefficient is large enough, two more extreme directions can appear. They are relicts of the two lost mirror planes of the tetragonal phase, but they have, however, non-crystallographic orientations in the orthorhombic phase.

We shall assume that the mentioned anisotropy of the free energy with respect to the angle φ arising from the crystal symmetry is not important in comparison with the influence of strains appearing inside the crystal in the low-temperature phase.

The spontaneous strain components can be obtained making use of the equilibrium equations $\partial f/\partial u_i = 0$:

$$\begin{aligned} u_1 &= l_1(p^2+q^2) - r_1[(\mathrm{d}_\zeta p)^2 + (\mathrm{d}_\zeta q)^2] - t_1(p^2+q^2)^2 - k_1 p^2 q^2 + \sigma_1 \Lambda_1 \\ u_2 &= u_1 \\ u_6 &= l_6(p^2-q^2) - r_6[(\mathrm{d}_\zeta p)^2 - (\mathrm{d}_\zeta q)^2] - t_6(p^2+q^2)(p^2-q^2) \\ &\quad - \tfrac{1}{2}s_6[(\mathrm{d}_\zeta p)^2 + (\mathrm{d}_\zeta q)^2]\sin(2\varphi) + \sigma_6 \Lambda_6 \end{aligned} \quad (7)$$

$$l_i = -\Lambda_i l_i' \qquad r_i = \Lambda_i r_i' \qquad t_i = \Lambda_i t_i' \qquad k_i = \Lambda_i k_i' \qquad s_6 = \Lambda_6 s_6'$$

where we set $\sigma_1 = \sigma_2$ and $\Lambda_1 = s_{11} + s_{12}$, $\Lambda_6 = s_{66}$; s_{ij} are elastic moduli. Substituting (7) into (1) and neglecting terms of order higher than 4, the density f is

$$f = \tfrac{1}{2}\alpha(p^2+q^2) + \tfrac{1}{4}\beta(p^2-q^2)^2 + \tfrac{1}{2}\gamma p^2 q^2 + \tfrac{1}{2}\kappa[(\nabla p)^2 + (\nabla q)^2] \quad (8)$$

in which β and γ are renormalized β' and γ'. Now it follows that the terms involving l_i, $i = 1, 6$, in formulae (7) are the only adequate terms with respect to the order of the expansion (8). Nevertheless, we show in the next section that the higher-order terms in (7) can lead to the temperature dependence of the APB orientation.

Finally, we shall assume a unidirectional modulation without topological defects, e.g. dislocations. Then the minimization of the free energy (8) should be carried out with the compatibility conditions taken into account. Such auxiliary conditions are of topological nature and, in fact, remove the isotropy of the free energy (8) with respect to the angle φ. In the two-dimensional case the compatibility conditions reduce to only one equation [13]:

$$2\partial^2_{xy} u_6(\zeta) = \partial^2_{yy} u_1(\zeta) + \partial^2_{xx} u_2(\zeta) \quad (9)$$

where the strain components are functions of ζ only. Making use of (5), the derivatives

in equation (9) can be written with respect to ζ and η, while tensor components are kept in x, y coordinate system:

$$\sin(2\varphi)\,\partial^2_{\zeta\zeta}u_6(\zeta) - \partial^2_{\zeta\zeta}u_2(\zeta) = 0. \tag{10}$$

The equations (7), (8) and (10) are the basic formulae of our further considerations.

3. Linear and rotational antiphase boundaries

Let us first examine an APB without strains taken into account. Then the density (8) should be considered without the auxiliary compatibility condition (10) and the free energy minimum corresponds to a *spontaneous* APB profile.

From the formula (8) four degenerate domain states follow: $(p_0, 0)$, $(-p_0, 0)$ and $(0, p_0)$, $(0, -p_0)$ with $p_0^2 = -t/\beta$. The first two possess the same strains (7) with the component $u_{xy} = l_6 p_0^2$; in contrast, the last two ferroelastic states possess strains with the shear component $u_{xy} = -l_6 p_0^2$. Hereafter we shall consider the APB with the following boundary conditions:

$$p(+\infty) = -p(-\infty) = p_0 \qquad \text{and} \qquad q(+\infty) = q(-\infty) = 0. \tag{11}$$

Then the spontaneous APB profile of the minimum free energy with the density (8) should be calculated making use of the Lagrange–Euler equations. Two types of APB exist. The *linear* one corresponds to the trivial solution and can be easily calculated setting $q(\zeta) \equiv 0$ (see e.g. [8]):

$$p(\zeta) = p_0 \tanh(K\zeta) \qquad q(\zeta) = 0 \qquad \text{where } p_0^2 = -t/\beta,\ K^2 = -t/2\kappa. \tag{12}$$

The mapping of the linear APB in the order parameter space is a straight line contour. When the solution (12) is unstable with respect to the linear vibrations of the q component then the *rotational* APB with $q(x) \not\equiv 0$ can exist.

The stable rotational boundary of finite width needs also the sixth-order terms in the expansion (8) (see [9], [10]). Nevertheless, the formulae (7) remain valid and are sufficient for our purposes. The spontaneous rotational APB profile has been solved analytically only in special cases [7–9]. Nevertheless, an approximate formula can be written (such a conclusion is supported by the analysis performed in [8–10]):

$$p(\zeta) = p_0 \tanh(K\zeta) \qquad q(\zeta) = \pm A \cosh^{-1}(K\zeta) \tag{13}$$

where K is defined in (12) and the amplitude A is an order parameter of the phase transition between the linear and the rotational structure. For $A = 0$ equations (13) give linear structure (12), while for $A > 0$ the two degenerate states of the rotational boundary follow. The qualitative difference between the linear and rotational structures is evident when looking at the strain tensor component u_6 in (7). Both APB structures have the same boundary conditions $u_6(-\infty) = u_6(+\infty) = l_6 p_0^2$ but in the centre of the linear structure $u_6(0) = 0$ while in the rotational case $u_6(0) = -l_6 A^2$ (we have neglected gradient terms in (7)). In the rotational boundary the sign of u_6 changes. This corresponds to the creation of a ferroelastic domain nucleus. When $A = p_0$ one of two saturated homogeneous states $p = 0$, $q = \pm p_0$ appears in the boundary centre and the APB splits fully into two ferroelastic walls.

The spontaneous value of the amplitude (order parameter) A corresponding to the spontaneous profile minimizing the free energy will be denoted A_s. In [8, 10] it was shown that the spontaneous amplitude A_s follows the Landau-type temperature dependence,

$A_s \sim (T_w - T)^{1/2}$, where T_w is the boundary transition temperature and $T_w < T < T_C$. Below T_w we have $A_s = 0$. Thus, the rotational boundary exists in the temperature interval $\Delta = T_C - T_w$. Further we construct for A_s a formula with the above-mentioned Landau dependence near T_w:

$$A_s = zp_0(1 - t^2/\Delta^2)^{1/2} \tag{14}$$

where $t = T - T_C$. Close to T_C ($t \to 0-$) we have $z = A_s/p_0$. The coefficient z measures the degree of saturation of the nucleus in the APB centre close to T_C. The transition in the APB occurs at $t = t_w = -\Delta < 0$.

The mapping of the rotational APB (13) in the order parameter space is an elliptic contour $p^2(\zeta)/p_0^2 + q^2(\zeta)/A^2 = 1$.

4. Strains in antiphase boundaries

Spontaneous linear and rotational structures were obtained in the preceding section. The spatial dependence of the spontaneous (plastic) strains is given by the formulae (7) setting $\sigma_i = 0$ and profiles (12) and (13) with the spontaneous amplitude A_s. We shall assume only compatible deformations. Then the compatibility condition (10) has to be fulfilled; consequently, the isotropy of the free energy (8) is removed and internal non-mechanical [14] stresses σ_1 and σ_6 can appear.

We shall start from the profile (13) in which both linear and rotational structures are involved. Substituting (13) into (7) the approximate formulae for the strain tensor components can be obtained:

$$u_1 = u_2 = L_1 p(\zeta)^2 + C_1 + \Lambda_1 \sigma_1 \qquad u_6 = \bar{L}_6 p(\zeta)^2 + C_6 + \Lambda_6 \sigma_6 \tag{15}$$

where L_1, $\bar{L}_6$, C_1 and C_6 are temperature-dependent coefficients that, up to $\bar{L}_6$, do not depend on φ. The calculation of L_1 and $\bar{L}_6$ and the proof of (15) are given in the appendix. The formulae for L_1 and $\bar{L}_6$ read:

$$L_1 = l_1 - l_1(A/p_0)^2 - g_1 t - h_1(A/p_0)^4 t$$

$$L_6 = l_6 + l_6(A/p_0)^2 - g_6 t + h_6(A/p_0)^4 t \qquad \bar{L}_6 = L_6 - g_a \sin(2\varphi)t \tag{16}$$

where $g_1 = r_1/2\kappa - t_1/\beta$, $g_6 = r_6/2\kappa - t_6/\beta$, $g_a = s_6/4\kappa$, $h_1 = t_1/\beta$ and $h_1 = t_1/\beta$.

Further we shall consider in general non-spontaneous APB profiles of the elliptic contour in the order parameter space given by equation (13) with the only degree of freedom A. In the preceding section A_s denotes the spontaneous value corresponding to the minimum free energy without considering the compatibility condition. For the sake of simplicity we shall assume that the internal stresses σ_i appear only due to the deviation of the amplitude A from its spontaneous value A_s. Then equations (15) can be written in the form:

$$\begin{aligned} u_1(A) &= u_2(A) = L_1(A)p(\zeta)^2 + C_1(A) \\ u_6(A) &= \bar{L}_6(A)p(\zeta)^2 + C_6(A) \end{aligned} \tag{17}$$

where A is, for the present, undetermined and the stresses σ^i follow from equation (17):

$$\sigma_i = \Lambda_i^{-1}[u_i(A) - u_i(A_s)] \qquad i = 1, 6$$
$$u_i(A) = u_i(A_s) + \Lambda_i \sigma_i. \tag{18}$$

The last equation in (18) is in fact that of (15). The elastic stresses are zero only if $A = A_s$. Finally, the compatibility equation (10) and the formulae (17) yield

$$\sin(2\varphi) = L_1(A)/\bar{L}_6(A) \tag{19}$$

or expressing $\bar{L}_6$ according to (16),

$$\sin(2\varphi) = 2(L_1/L_6)/\{1 + [1 - 4(L_1/L_6)(g_a/L_6)t]^{1/2}\}. \tag{20}$$

The expressions (20) and (16) determine the temperature dependence of the APB orientation. The solution has two branches, upper one $\varphi_1(t)$ and lower one $\varphi_2(t) = \pi/2 - \varphi_1(t)$. These branches join each other when $L_1 = \bar{L}_6$.

Let us first consider the linear APB, which does not undergo transformation into the rotational structure. Then the spontaneous amplitude A_s is equal to zero. Three examples of the upper branches $\varphi_1(t)$ are shown in figure 2, while the lower branches $\varphi_2(t) = \pi/2 - \varphi_1(t)$ are not depicted in the figure. Nevertheless, the lower branch $\varphi_2(t)$ can be constructed by reflecting $\varphi_1(t)$ in the t axis. The curve 'a' has a straight-line part above t_r corresponding to the single solution of equation (19) with the non-zero amplitude $A \neq A_s = 0$, while below t_r the amplitude has its spontaneous value $A = A_s = 0$.

In order to discuss the solutions of equation (19) in more detail, we shall construct the strain ellipse and look at its variation across the boundary. The equation of the ellipse is obtained from (15) as

$$[(L_1 + \bar{L}_6)p^2(\zeta) + C_1 + C_6]\mu^2 + [(L_1 - \bar{L}_6)p^2(\zeta) + C_1 - C_6]\nu^2 = 1 \tag{21}$$

where μ, ν are principal axes rotated through $\pi/4$ relative to x, y. Three cases are possible:

(i) $L_1 < \bar{L}_6$ and $A = A_s = 0$ (figure 3(a)). For each point ζ an ellipse (21) can be constructed. One can easily show that all such ellipses (two of them are shown in figure 3(a)) intersect at four invariant points A, B, C, D. Then the APB planes are depicted by two dotted lines AB, CD and two plane normals, ζ_1, ζ_2 contain with the x axis the angles φ_1, φ_2, respectively. These angles are two solutions of equation (19) symmetrically distributed around $\varphi = \pi/4$. Let us choose one $\varphi_1(t)$ curve, e.g. the 'a' curve, in figure 2. Then this regime ($L_2 < \bar{L}_6$) occurs for $t < t_r$. The lower branch $\varphi_2(t) = \pi/2 - \varphi_1(t)$ is not depicted.

The boundary profile is given by (12), i.e. the amplitude $A = A_s = 0$ has spontaneous zero value, and no additional deformations are needed. The elastic stress is zero according to (18) and the boundary is stress-free.

(ii) $L_1 = \bar{L}_6$ and $A = A_s = 0$ (figure 3(b)). All ellipses (21) touch at two invariant points A, B and the dotted line CD represents a single boundary plane. Its normal ζ contains with the x axis the angle $\varphi = \pi/4$, which is the only solution of equation (19). For the curve 'a' in figure 2 this holds at $t = t_r$, where $\varphi_1(t_r) = \varphi_2(t_r) = \pi/4$ and both branches merge.

The boundary is still stress-free since its profile (12) has not been modified, but, contrary to the above case, only one possible orientation exists. The amplitude A has its spontaneous zero value, i.e. $A = A_s = 0$.

(iii) $L_1 > \bar{L}_6$ when $A = A_s = 0$ (figure 3(c)). This case is qualitatively different. Equation (19) has no solution for $A = A_s = 0$. Then any two ellipses (21) do not intersect,

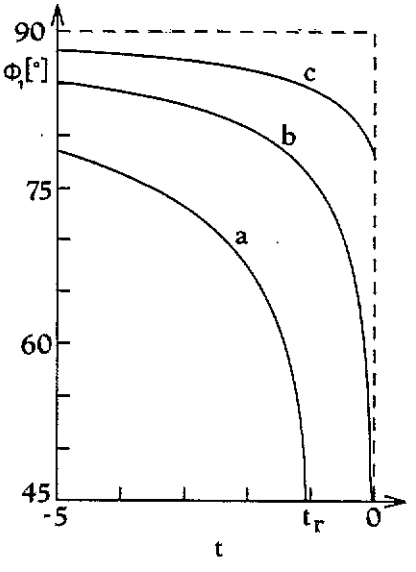

Figure 2. The temperature dependence of the orientation angle φ_1 of the linear APB. The lower branch $\varphi_2 = \pi/2 - \varphi_1$ is not depicted. Curve 'a': $l_1 = 2.9$, $l_6 = 1$, $g_1 = 0$, $g_6 = 1$, $g_a = 3$. For $t \leqslant t_r$ the APB is stress-free; for $t_r < t < 0$ the strained APB appears locked in $\varphi = \pi/4$. Curve 'b': $l_1 = 1.1$, $l_6 = 1$, $g_1 = 0$, $g_6 = 1$, $g_a = 3$. Curve 'c': $l_1 = 0.4$, $l_6 = 1$, $g_1 = 0$, $g_6 = 1$, $g_a = 3$. Only stress-free boundaries appear in 'b' and 'c'.

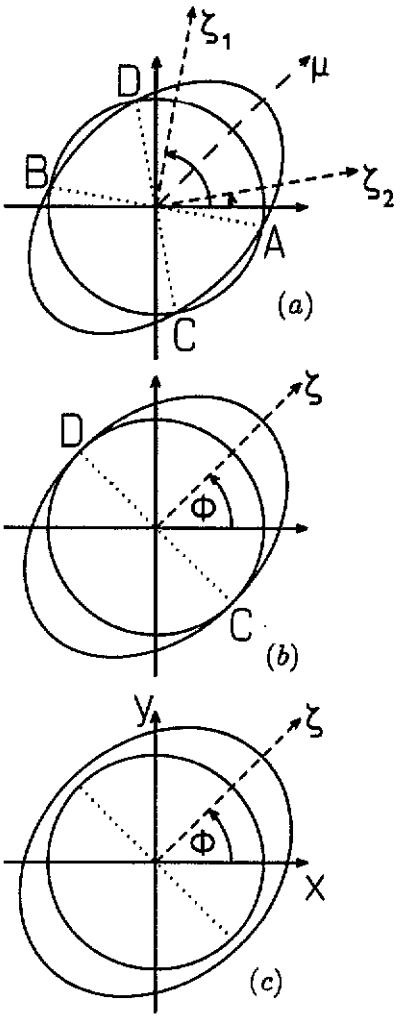

Figure 3. Strain ellipses corresponding to equation (21). (*a*) All ellipses (21) intersect at four points A, B, C, D; only two of them are shown. AB and CD are the APB planes; their normals ζ_1, ζ_2 contain with the x axis angles φ_1, φ_2, respectively. Equation (13) has two solutions φ_1, φ_2 and the APB are stress-free. (*b*) All ellipses (21) touch at two points C, D, and the angle $\varphi = \pi/4$ is the only solution of equation (13). The APB normal ζ coincides with the principal axis μ of the strain ellipses. (*c*) All ellipses (21) do not intersect and equation (13) has no solution. The APB is strained and locked at $\varphi = \pi/4$.

the spontaneous profile (12) is not adequate and an additional deformation is needed in order to satisfy the compatibility conditions. The new compatible profile has to satisfy equation (19). Then its amplitude A is the solution of the equation

$$L_1(A) = \bar{L}_6(A) \tag{22}$$

which is, in fact, a consequence of the compatibility restriction. The explicit formula for A could be easily obtained from (22) and we do not write it here. The equation (22), from which the amplitude A ought to be calculated, corresponds to a deformation of ellipses in figure 3(c) until they touch at two points C, D as depicted in figure 3(b). The orientation is locked in the crystallographic value $\varphi = \pi/4$. The boundary plane is represented by the dotted line in figure 3(c) for the incompatible APB and in figure 3(b) for the compatible one. For the curve 'a' in figure 2 this situation occurs for $t > t_r$. Then the amplitude A decreases according to equation (22) from its maximum value at $t = 0$ to the spontaneous zero value at $t = t_r$.

The boundary is strained even in the orientation with minimum energy. It means that the non-mechanical stress (see e.g. [14]) appears along the APB plane according to (18) since $A \neq A_s$. The compatible profile is the rotational one (13), where the amplitude A is obtained from equation (22). The full deformation $u_i(A)$ of the strained APB now consists of the plastic $u_i(A_s)$ and the elastic u_i^e parts: $u_i(A) = u_i(A_s) + u_i^e$, $u_i^e = \Lambda_i \sigma_i$ (see equation (18)).

Till now we have discussed the APB orientations with minimum energy. Nevertheless, other orientations possessing higher energy can also appear, though with lower probability, and the APB pattern can consist of complicated curved lines or loops. Two limiting cases are instructive. If the boundary energy possesses only small anisotropy then one can expect a nearly isotropic APB pattern. On the other hand, large anisotropy leads to patterns with clearly preferred orientations, either two non-crystallographic ones with angles φ_1 and φ_2 (figure 3(a)) or one crystallographic orientation with $\varphi = \pi/4$ (figures 3(b) and (c)). Finally, one can also conclude that the APB of an orientation with higher energy has rotational structure since the amplitude A is necessarily non-zero.

In summary the strained APB locked at the crystallographic orientation $\varphi = \pi/4$ ($L_1(A) = \bar{L}_6(A)$ only if $A \neq 0$) has rotational structure with A given by (22) and $A \neq A_s = 0$. It becomes a stress-free APB with linear structure ($A = A_s = 0$) when $L_1(0) = \bar{L}_6(0)$, and for $L_1(0) < \bar{L}_6(0)$ takes one of two degenerate orientations φ_1, φ_2. In the limit $L_1/\bar{L}_6 \to 0$ these orientations approach crystallographic values $\varphi_1 = 0$, $\varphi_2 = \pi/2$.

The linear APB without transition into the rotational structure was discussed above. Now, let us assume the occurrence of such transition at t_w, i.e. $T_w < T_C$. Then the formula for the angle φ versus temperature dependence can be directly obtained. First, substituting the spontaneous amplitude A_s from equation (14) into (16) two expressions follow:

$$\begin{aligned} L_1 &= l_1 - l_1 z^2(1 - t^2/\Delta^2) - g_1 t - h_1 z^4(1 - t^2/\Delta^2)^2 t \\ L_6 &= l_6 + l_6 z^2(1 - t^2/\Delta^2) - g_6 t + h_6 z^4(1 - t^2/\Delta^2)^2 t. \end{aligned} \tag{23}$$

Finally, the orientation versus temperature dependence is determined by (20) and (23). The solution has two branches, upper one $\varphi_1(t)$ and lower one $\varphi_2(t) = \pi/2 - \varphi_1(t)$. Three representative examples of the $\varphi_1(t)$ curve (upper branch) are shown in figure 4. In comparison with the linear case in figure 2, a minimum on the $\varphi_1(t)$ curve can appear at $t = t_w$ (curves 'b' and 'c'). This minimum has the following meaning. Decreasing t from 0 to t_w (i.e. decreasing T from T_C to T_w), the new domain nucleus in the APB centre is pushed out and the amplitude $A = A_s$ given by (14) decreases to zero. At t_w the rotational structure is transformed to the linear one since $A = A_s = 0$. Thus the minimum in figure 4 corresponds to the phase transition of the APB structure. The curves 'b' and 'c' do not

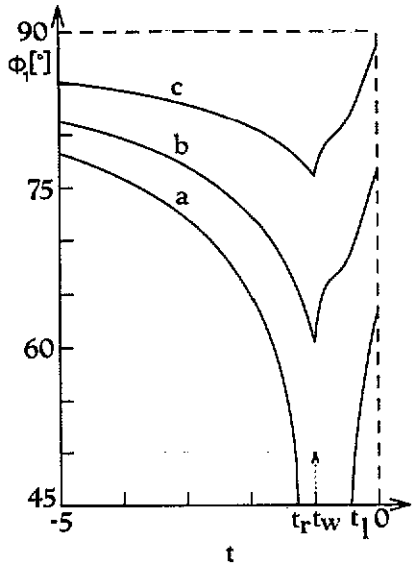

Figure 4. The temperature dependence of the orientation angle φ_1 of the APB undergoing transition between the linear and rotational structure. The parameters are: $l_6 = 1, g_1 = 0, g_6 = 1, h_1 = 1$, $h_6 = 1$, $z = 1$; and for curve 'a', $l_1 = 2.6$, $g_a = 1$; for curve 'b', $l_1 = 1.9$, $g_a = 1$; for curve 'c', $l_1 = 1.1$, $g_a = 3$. The transition temperature is t_w. The straight-line part of curve 'a' corresponds to the strained APB.

reach the t axis and so the APB structure is stress-free all times, since in such a case equation (19) has a solution for the spontaneous amplitude A_s. Curve 'a' shows a more complicated situation. The stress-free rotational structure with $A = A_s$ (given by equation (14)) occurs above t_1. In the range $t_r < t < t_1$ the APB possesses the strained rotational structure with $A \neq A_s$, where A is the solution of equation (22). Below t_r the APB becomes linear and stress-free with $A = A_s = 0$. The temperature t_r has the same sense in figures 2 and 4.

5. Conclusions

We have studied the APB in the improper ferroelastic crystal Hg_2Cl_2 in the framework of the Landau theory. The results of our analysis are valid also for improper ferroelastic substances with the same form of the free energy, e.g. KSCN, and qualitatively also for other crystals with the transition from tetragonal to orthorhombic phase, even if they have different free energy expansion, e.g. $Gd_2(MoO_4)_3$.

The spontaneous order parameter induces spontaneous deformation of each small piece of the crystal inside the boundary. If the mutual compatibility of the spontaneous deformations is satisfied for an appropriately oriented APB without any additional deformations, then such an APB is stress-free and has minimum energy in the crystal. Nevertheless, other orientations with lower probability can also occur. The preference of a non-crystallographic APB orientation, but with frequent occurrence of all others, was observed in GMO by Meleshina *et al* [1]. We have calculated the most probable APB orientation versus temperature dependence. The obtained curve 'b' in figure 2 is in good agreement with measurements performed by Barkley and Jeitschko [3].

of the minimum energy and the compatible APB is forced to possess rotational structure. Then a stress exists in the boundary plane which can lead to the creation of topological defects in a long enough APB. The strained boundary orientation is locked in the crystallographic position, and in the case of high anisotropy of the free energy with respect to the APB orientation we expect the APB to be oriented in the crystal practically only at this lock-in orientation. The strained APB cannot be very long. In the KSCN crystal Schranz *et al* [15] observed etch lines consisting of short grooves in the crystallographic direction. The authors interpreted them as APB. They are possible candidates of the strained boundaries which we have predicted above.

Both structures are present in the 'a' curve of figure 2. The strained boundary of the rotational structure exists for $t_r < t < 0$ and the stress-free linear one appears for $t \leqslant t_r$. Thus the APB is released at t_r.

The rotational structure of the APB was theoretically predicted by several authors [8–10] and the possibility of transition between linear and rotational boundaries was pointed out. We have shown that this transition can manifest itself by an appearance of the minimum in the preferred APB orientation versus temperature dependence. Then the APB structure can be distinguished: the linear one occurs for $t \leqslant t_w$ and the rotational one for $t > t_w$. Such a phenomenon has not been experimentally observed so far.

Finally we conclude that further measurements would be desirable to confirm our theory. Knowledge of the boundary orientation versus temperature dependence in KSCN would resolve the problem of whether the observed grooving in KSCN [15] really consists of strained APB. Also measurements of the APB internal deformations would be desirable. An attempt to observe the APB in Hg_2Cl_2 would be interesting since they have not been detected so far in these crystals.

We have presented the two-dimensional theory with respect to deformations, which is simple enough to obtain analytic expressions for the APB compatible profile and the formulae for its most probable orientation in the crystal. Our results are closely related to experimental observations and they allow one to classify the APB patterns in crystals. We have shown that sometimes non-mechanical internal stresses can appear inside the APB. We expect that the two-dimensional approach is relevant in such cases when the most important deformations near T_C are those in one plane. Such candidates are crystals with uniaxial elastic anisotropy in the high-temperature phase (tetragonal symmetry), extreme examples of which are mercurous halides. The two-dimensional approximation can fail for crystals in which deformations along all three directions are of importance near T_C. Such a situation can occur, e.g. in perovskite-type compounds like $SrTiO_3$, with cubic symmetry above T_C. Then a three-dimensional model has to be used as was pointed out in [11].

Acknowledgments

The author thanks Dr F Kroupa and Dr O Hudak for many helpful comments and also wishes to thank Dr V Janovec for his encouragement and many stimulating discussions.

Appendix

The calculation of L_1, $\bar{L}_6$ and the proof of equations (13) are presented. For the profile (13) the following identities are valid:

$$p^4(\zeta) = p_0^2 p^2(\zeta) - o(\zeta) \qquad \text{where } o(\zeta) = p_0^4[\tanh^2(K\zeta) - \tanh^4(K\zeta)] \tag{A1}$$

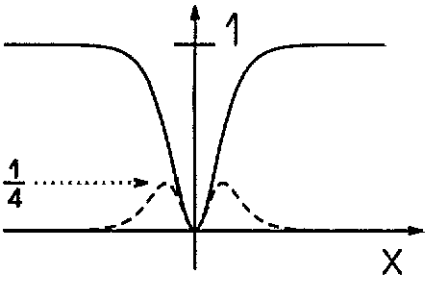

Figure 5. In the appendix equation (A1) reads: $p(x)^4 = p_0^2 p(x)^2 - o(x)$. The function $o(x)$ (broken curve) is small in comparison with the function $p_0^2 p(x)^2$ (full curve). Both functions depicted are divided by p_0^4.

$$(d_\zeta p)^2 = -K^2 p^2(\zeta) + p_0^2 K^2 - \iota(\zeta)$$

$$\text{where } \iota(\zeta) = p_0^2 K^2 [\cosh^{-2}(K\zeta) - \cosh^{-4}(K\zeta)]. \tag{A2}$$

Similar identities are also valid for $q^4(\zeta)$, $(d_\zeta q)^2$, $q^2(\zeta)$ and $p^2(\zeta)q^2(\zeta)$, which are involved in (7). A comparison of the leading term $p_0^2 p^2(\zeta)$ and the function $o(\zeta)$ in (A1) is displayed in figure 5. The ratio of the maximum value of $o(\zeta)$ and the maximum of $p_0^2 p^2(\zeta)$ is $\frac{1}{4}$. A similar relation holds also for (A2). We can, therefore, treat o and ι as small functions.

Using the above identities, each term in equations (7) can be written in the form

$$Cp^2(\zeta) + B + \sigma(\zeta) \tag{A3}$$

where C, B are constants and $\sigma(\zeta)$ is small relative to $Cp^2(\zeta)$. Then the summation in (7) gives

$$\begin{aligned} u_1 = u_2 &= L_1 p(\zeta)^2 + C_1 + \mathcal{O}_1(\zeta) + \Lambda_1 \sigma_1 \\ u_6 &= \bar{L}_6 p(\zeta)^2 + C_6 + \mathcal{O}_6(\zeta) + \Lambda_6 \sigma_6 \end{aligned} \tag{A4}$$

where L_1, $\bar{L}_6$ are renormalized parameters l_1, l_6, and $\mathcal{O}_1$, $\mathcal{O}_6$ are small functions that can be neglected. The formulae for L_1 and $\bar{L}_6$ are given by the formulae (16). In a similar way also coefficients C_1 and C_6 could be expressed as functions of the amplitude A and temperature t, but they are not of interest to us here.

References

[1] Meleshina V A, Indenbom V L, Bagdasarov Kh S and Polkhovskaya T M 1973 *Kristallografiya* **18** 1218 (1974 *Sov. Phys.–Crystallogr.* **18** 764)
[2] Janovec V 1976 *Ferroelectrics* **12** 43
[3] Barkley J R and Jeitschko W 1973 *J. Appl. Phys.* **44** 938
[4] Yamamoto N, Yagi K and Honjo G 1977 *Phys. Status Solidi* a **44** 147
[5] Capelle B and Malgrange C 1982 *J. Appl. Phys.* **53** 6762
[6] Capelle B and Malgrange C 1984 *J. Physique* **45** 1827
[7] Ishibashi Y and Dvorak V 1976 *J. Phys. Soc. Japan* **41** 1650
[8] Lajzerowicz J and Niez J J 1978 *Solitons and Condensed Matter Physics* ed A R Bishop and T Schneider (Berlin: Springer) p 195
[9] Sonin E B and Tagancev A K 1989 *Ferroelectrics* **98** 291
[10] Bullbich A A and Gufan Yu M 1989 *Ferroelectrics* **98** 277
[11] Cao W and Barsch G R 1990 *Phys. Rev.* B **41** 4334
[12] Barta C, Kaplyanskij A A, Kulakov B B, Malkin B Z and Markov Yu F 1976 *Zh. Eksp. Teor. Fiz.* **70** 1429
[13] Fung Y C 1965 *Foundations of Solid Mechanics* ed Y C Fung (Englewood Cliffs, NJ: Prentice-Hall)
[14] Anthony K H 1970 *Fundamental Aspects of Dislocation Theory* ed J A Simmons, R de Wit and R Bullough, Nat. Bur. Stand. Spec. Publ. 317, vol I, p 637
[15] Schranz W, Streuselberger T, Fuith A, Warhanek H and Götzinger M 1988 *Ferroelectrics* **88** 136